Available online at www.sciencedirect.com
ScienceDirect
Polymer 48 (2007) 5355–5368
polymer
www.elsevier.com/locate/polymer

Synthetic 6FDA–ODA copolyimide membranes for gas separation and pervaporation: Functional groups and separation properties

Shude Xiao, Robert Y.M. Huang*, Xianshe Feng

Department of Chemical Engineering, University of Waterloo, Waterloo, ON, Canada N2L 3G1

Received 12 June 2007; received in revised form 5 July 2007; accepted 8 July 2007
Available online 13 July 2007

Abstract

Copolyimides were prepared from one-step polymerization of 6FDA and ODA with four diamines DBSA, DABA, DAPy and DANT as the third monomers. Polymers were characterized with GPC, FTIR, NMR, DSC and TGA. Surface free energies and membrane–water interfacial free energies were calculated from contact angles, and results indicated that DABA, DBSA and DAPy moieties helped to increase the hydrophilicity. Gas permeation was measured for N_2, O_2, H_2, He and CO_2. Linear moiety contribution method was proposed to study the moiety effects on gas selectivities. The selectivities of O_2/N_2, H_2/N_2, and He/N_2 were greatly affected by the steric effects from the monomer moieties, but permeation of CO_2 was controlled by its solubility in polymers as well as the interactions with the functional groups. Water permeation and dehydration of isopropanol were carried out in pervaporation processes. Concentration coefficients were proposed for feed concentration effects on permeation flux, and permeation activation energies were used to study the temperature dependence of flux. Linear moiety contribution method was applied to quantitatively compare the effects of monomer moieties. Functional groups could change the sorption and diffusion properties in pervaporation, and moiety contribution factors indicated that feed concentrations mainly affected sorption properties, whereas temperatures influenced diffusion properties.

Keywords: Polyimide; Gas separation; Pervaporation dehydration

1. Introduction

Polyimide membranes, benefiting from their superior physiochemical and mechanical properties, received continuous research interest from industries and academia. From the statistical analysis, 47% of polyimide membranes are used in gas separation and around 5% in pervaporation processes [1]. Some affordable polyimide materials are commercially available in the market [2–4]. However, tailored polymers are necessarily needed to meet the requirement of specific applications, such as pervaporation and gas separations in membrane technologies [5]. Researchers are working on molecular designing and modification of polyimides to improve the separation selectivity as well as the permeation flux. Synthesis of new polyimides and incorporation of functional groups (such as sulfonic acid and carboxylic acid groups) and bulky side groups in the wholly aromatic polyimides have been attempted as research directions [6,7].

For gas permeation membranes, side groups such as sulfonic acid and methyl groups were introduced into the polyimide main chains, and their influences on gas permeation properties were discussed in some work. Piroux et al. [8] prepared sulfonated polyimides from 1,4,5,8-naphthalene tetracarboxylic dianhydride (NTDA), 4,4′-diamino-2,2′-biphenyl disulfonic acid (BDSA) and some non-sulfonated diamines, but the gas permeation properties were found to be greatly dependent on the structures of the non-sulfonated diamines of the copolyimides. To reveal the effects of sulfonic acid groups on membrane properties, Tanaka et al. [9] synthesized polyimides from NTDA and 2,2-bis[4-(4-aminophenoxy)phenyl]-hexafluoropropane disulfonic acid, and a comparison was made on their gas permeabilities with those of the non-sulfonated polyimides having the same backbone structure, which showed that the sulfonated polyimide had higher

* Corresponding author. Tel.: +1 519 888 4567x33399.
E-mail address: ryhuang@uwaterloo.ca (R.Y.M. Huang).

0032-3861/$ - see front matter © 2007 Elsevier Ltd. All rights reserved.
doi:10.1016/j.polymer.2007.07.010

selectivity of H_2 over CH_4 without loss of H_2 permeability. Al-Masri et al. [10] prepared polyimide membranes from methyl-substituted diamine monomers and the gas permeation properties suggested that introduction of methyl groups into the polymer main chains created large free volume for gas transport. Pinel et al. [11] synthesized polyimides with trifluoromethyl and methoxyl side groups, and studies showed that chain cohesion properties were decreased and the available void space for diffusion of gas molecules was increased by the trifluoromethyl substituents, but the methoxyl substituents did not show significant steric effects on gas permeations.

Polyimides with functional groups were also prepared for pervaporation membranes. However, based on the difference between gas separation and pervaporation, the same substituents may act in different ways to affect the separation properties of the membranes. Kang et al. [7] used 3,5-diaminobenzoic acid (DABA) to hydrophilically modify the polyimide from pyromellitic dianhydride (PMDA) and 4,4′-oxydianiline (ODA), and it was discovered that higher flux and higher selectivity of water/ethanol were achieved, resulting from the hydrogen bonding between water and the carboxylic acid in DABA, and further study showed that it was the diffusivity of the penetrants that determined the pervaporation performance, other than the solubility. Xu et al. [12] investigated the effect of DABA contents in the polymer main chains of polyimides synthesized from 4,4′-(hexafluoroisopropylidene)-diphthalic anhydride (6FDA) and 4,6-trimethyl-1,3-phenylenediamine (DAM) for pervaporation separation of toluene/isooctane mixtures, and it was concluded that the polarity of DABA promoted membrane selectivity, but the smaller size of DABA and the interaction between carboxylic acid and polymer main chains decreased the fractional free volume and facilitated packing of the segmental chains, which finally caused a reduction of membrane swelling together with an improvement in diffusivity selectivity.

Since pervaporation and gas separation processes follow the solution-diffusion mechanism, it is reasonable to investigate how the functional groups and monomer structures behave in the mass transport of both gas permeation and pervaporation, and to find out to what extent they may change the permeability and selectivity of the membranes. Therefore, based on the similarity of the monomer structures and the differences between the functional groups, diamine monomers with pyridine and naphthalene moieties and monomers with side groups (sulfonic acid and carboxylic acid groups) were used in the preparation of copolyimides. Gas separation and pervaporation properties of the polyimides were investigated and contributions from diamine monomers were quantitatively revealed and discussed.

2. Experimental

2.1. Materials

4,4′-(Hexafluoroisopropylidene)diphthalic anhydride (6FDA, m.p. 246 °C, >98%) was provided by TCI. 4-Aminophenyl ether (ODA, m.p. 189–193 °C, 98%), 2,4-diaminobenzenesulfonic acid (DBSA, 97%), 3,5-diaminobenzoic acid (DABA, m.p. 235 °C, 98%), 2,6-daminopyridine (DAPy, m.p. 115–123 °C, 98%), 1,5-diaminonaphthalene (DANT, m.p. 187–190 °C, 97%), *m*-cresol (b.p. 203 °C, 97%), isoquinoline (m.p. 242 °C, 97%), tetrahydrofuran (THF, b.p. 66 °C, 99.5%) and pyridine (b.p. 115–116 °C, >99%) were obtained from Acros Organics. Glycerol (SigmaUltra grade, ≥99%), formamide (SigmaUltra grade, ≥99%) and diiodomethane (Reagent-Plus® grade, ≥99%), ethanol (b.p. 78 °C, 99.5%), isopropanol (anhydrous, b.p. 82 °C, 99.5%) were purchased from Sigma–Aldrich. Deionized water (≤2 μS/cm) was provided by the Department of Chemical Engineering, University of Waterloo. DAPy was recrystallized from water/ethanol followed by drying *in vacuo*. Other reagents and materials were used directly as received.

2.2. Characterization

Differential scanning calorimetry (DSC) analysis was run on TA Instruments Model DSC 2920 Differential Scanning Calorimeter and thermogravimetric analysis (TGA) was performed on TA Instruments Model SDT 2960 Simultaneous DSC–TGA. Samples were dried *in vacuo* at 120 °C overnight before thermal analyses. DSC thermograms were recorded from 250 to 370 °C at a heating rate of 10 °C/min under the protection of helium. DSC baseline was obtained from running DSC with the empty aluminum sample pan. TGA curves were plotted by heating the samples from 100 to 650 °C at a heating rate of 10 °C/min in a helium atmosphere. Fourier transform infrared (FTIR) spectroscopy was carried out with Bio-Rad Excalibur 3000MX spectrometer for polymer films cast on NaCl crystals. Gel permeation chromatography (GPC) was conducted to obtain molecular weights and molecular weight distributions using Waters GPC system with DAWN® DSP-F Laser Photometer, Waters 2410 Refractive Index Detector, and 3 PL gel 10 μm Mixed-B columns (300 × 7.5 mm). The GPC was calibrated with polystyrene standards and THF was used as the eluent. Nuclear magnetic resonance (NMR) spectroscopy was performed with Bruker 300 MHz NMR to record ^1H and ^{19}F NMR spectra with pyridine-d_5 as the solvent. Tantec Contact Angle Meter (U.S. Patent 5,268,733) was used to obtain the images of contact angles for membranes with water, glycerol, formamide and diiodomethane at room temperature.

2.3. One-step polymerization

Monomers used in this work are shown in Fig. 1. Polyimides (shown in Table 1) were synthesized by one-step polymerization (Fig. 2) and the procedures are outlined as follows, 6FDA–8ODA–2DAPy as an example.

6FDA (1.795 g, 4.0 mmol), ODA (0.654 g, 3.2 mmol), and DAPy (0.088 g, 0.8 mmol) were charged into a 100 mL three-necked flask equipped with a mechanical stirrer, a Dean–Stark trap, a condenser and nitrogen inlet/outlet. *m*-Cresol (12.5 mL) was added into the flask to afford a concentration of 20 w/v %, and extra *m*-cresol (1.5 mL) and a catalytic amount of

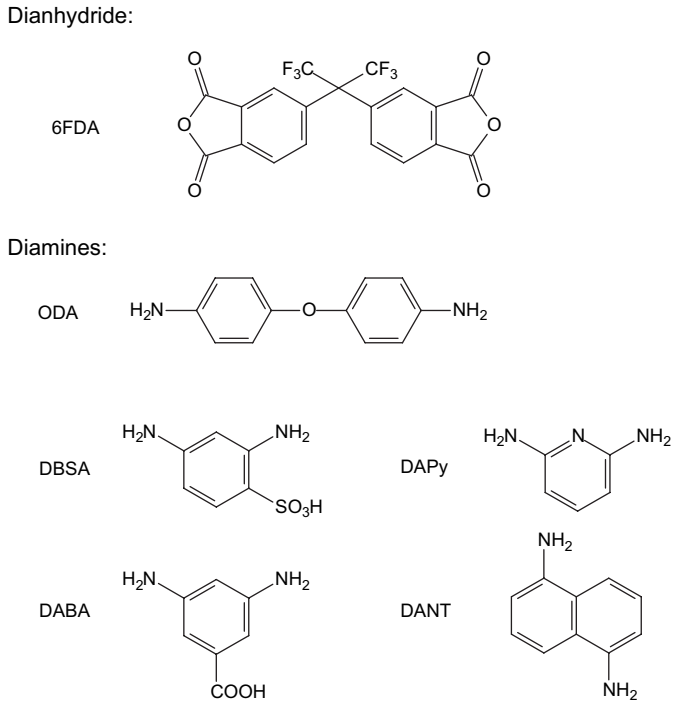

Fig. 1. Monomers of polyimides.

isoquinoline were also charged into the system. The solution reacted at 75 °C for 2 h and then the temperature was slowly increased to 185 °C. Polymerization lasted for 20–24 h, and during this course, *m*-cresol (1.5 mL) was distilled out through the trap. The viscous solution was cooled below 120 °C and then precipitated into an excess of ethanol to get the white polymer. The polymer was collected and washed with ethanol in a Soxhlet extractor for at least 10 h to extract *m*-cresol. The final product 6FDA–8ODA–2DAPy was dried *in vacuo* at 150 °C for 20 h.

6FDA–ODA (film, cm^{-1}): 3490 (vw) ν_{as} N–H, 3054 (br, w) aromatic δ C–H, 1785 (m) ν_{as} C=O, 1728 (s) ν_s C=O, 1597 (w) phenyl ring, 1502 (s) phenyl ring, 1379 (m) ν C–N, 1299 (m) ν_s CF_3, 1245 (m) ν_{as} C–O–C, 1113 (br, m) imide, 1015 (w) aromatic ring, 723 (m) δ imide. ^{1}H NMR (pyridine-d_5, δ ppm): 8.17–8.14 (4H), 8.06–8.04 (2H), 7.91 (d, $J = 9$ Hz, 4H), 7.31 (d, $J = 9$ Hz, 4H). ^{19}F NMR (pyridine-d_5, δ ppm): 61.46.

6FDA–8ODA–2DBSA (film, cm^{-1}): 3490 (vw) ν_{as} N–H, 3070 (br, w) aromatic δ C–H, 1785 (m) ν_{as} C=O, 1727 (s) ν_s C=O, 1598 (w) phenyl ring, 1501 (s) phenyl ring, 1380 (m) ν C–N, 1299 (m) ν_s CF_3, 1243 (m) ν_{as} C–O–C, 1112 (br, m) imide, 1015 (w) aromatic ring, 722 (m) δ imide. ^{1}H NMR (pyridine-d_5, δ ppm): 8.52 (0.2H), 8.17–8.04 (6.4H), 7.92–7.90 (3.2H), 7.33–7.30 (3.2H).

6FDA–6ODA–4DBSA (film, cm^{-1}): 3494 (vw) ν_{as} N–H, 3071 (br, w) aromatic δ C–H, 1785 (m) ν_{as} C=O, 1728 (s) ν_s C=O, 1602 (w) phenyl ring, 1502 (s) phenyl ring, 1381 (br, m) ν C–N, 1298 (m) ν_s CF_3, 1257 (br, m) ν_{as} C–O–C, 1111 (br, m) imide, 1015 (w) aromatic ring, 721 (m) δ imide. ^{1}H NMR (pyridine-d_5, δ ppm): 8.51 (0.3H), 8.17–8.04 (6.8H), 7.92–7.90 (2.4H), 7.33–7.30 (2.4H).

6FDA–8ODA–2DABA (film, cm^{-1}): 3496 (vw) ν_{as} N–H, 3071 (br, w) aromatic δ C–H, 1786 (m) ν_{as} C=O, 1730 (s) ν_s C=O, 1599 (w) phenyl ring, 1502 (s) phenyl ring, 1381 (m)

Table 1
6FDA–ODA copolyimides and their molecular weights

Polyimides	Monomers	Molar ratio	$\overline{M}_n$	$\overline{M}_w$	$\overline{M}_w/\overline{M}_n$	$\overline{DP}$
6FDA–ODA	6FDA:ODA	1:1	84,150	89,070	1.06	138
6FDA–8ODA–2DBSA	6FDA:ODA:DBSA	1:0.8:0.2	140,200	205,800	1.47	231
6FDA–6ODA–4DBSA	6FDA:ODA:DBSA	1:0.6:0.4	152,800	165,700	1.08	253
6FDA–8ODA–2DABA	6FDA:ODA:DABA	1:0.8:0.2	62,750	89,650	1.43	105
6FDA–6ODA–4DABA	6FDA:ODA:DABA	1:0.6:0.4	125,600	166,600	1.33	213
6FDA–9ODA–1DAPy	6FDA:ODA:DAPy	1:0.9:0.1	34,560	48,470	1.40	57
6FDA–8ODA–2DAPy	6FDA:ODA:DAPy	1:0.8:0.2	28,690	37,050	1.30	48
6FDA–9ODA–1DANT	6FDA:ODA:DANT	1:0.9:0.1	63,730	72,780	1.14	105
6FDA–8ODA–2DANT	6FDA:ODA:DANT	1:0.8:0.2	82,110	90,560	1.10	137

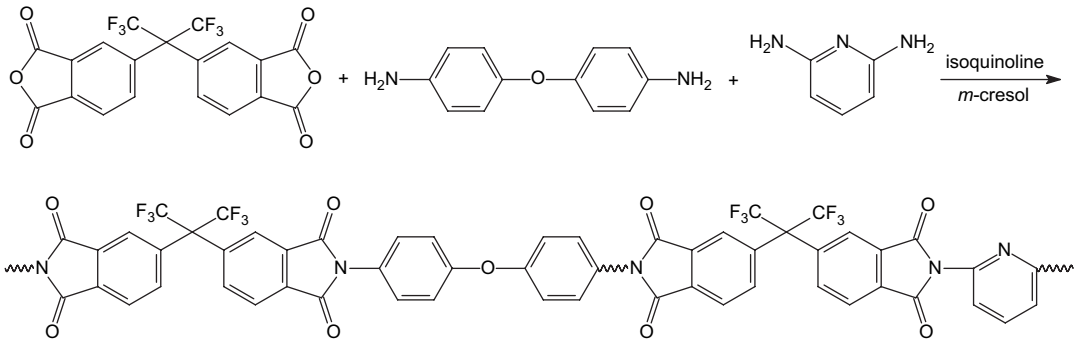

Fig. 2. One-step polymerization of 6FDA–8ODA–2DAPy.

ν C–N, 1298 (m) ν_s CF_3, 1247 (br, m) ν_{as} C–O–C, 1111 (br, m) imide, 1015 (w) aromatic ring, 723 (s) δ imide. ^{1}H NMR (pyridine-d_5, δ ppm): 8.98–8.97 (0.3H), 8.18–8.04 (6.2H), 7.93–7.90 (3.2H), 7.33–7.30 (3.2H).

6FDA–6ODA–4DABA (film, cm^{-1}): 3494 (vw) ν_{as} N–H, 3034 (br, w) aromatic δ C–H, 1784 (m) ν_{as} C=O, 1728 (s) ν_s C=O, 1599 (w) phenyl ring, 1502 (s) phenyl ring, 1383 (br, m) ν C–N, 1300 (m) ν_s CF_3, 1244 (br, m) ν_{as} C–O–C, 1102 (br, m) imide, 1015 (w) aromatic ring, 721 (m) δ imide. ^{1}H NMR (pyridine-d_5, δ ppm): 8.98–8.97 (0.6H), 8.20–8.04 (6.4H), 7.92–7.89 (2.4H), 7.33–7.30 (2.4H).

6FDA–8ODA–2DAPy (film, cm^{-1}): 3494 (vw) ν_{as} N–H, 3081 (br, w) aromatic δ C–H, 1786 (m) ν_{as} C=O, 1728 (s) ν_s C=O, 1595 (w) aromatic ring, 1502 (s) aromatic ring, 1380 (m) ν C–N, 1298 (m) ν_s CF_3, 1243 (br, m) ν_{as} C–O–C, 1113 (br, m) imide, 1015 (w) aromatic ring, 723 (s) δ imide. ^{1}H NMR (pyridine-d_5, δ ppm): 8.17–8.01 (6.3H), 7.93–7.90 (3.2H), 7.33–7.30 (3.2H), ~7.32 (theoretically 0.2H, overlapped).

6FDA–9ODA–1DAPy (film, cm^{-1}): 3493 (vw) ν_{as} N–H, 3070 (br, w) aromatic δ C–H, 1785 (m) ν_{as} C=O, 1728 (s) ν_s C=O, 1596 (w) aromatic ring, 1501 (s) aromatic ring, 1380 (m) ν C–N, 1297 (m) ν_s CF_3, 1245 (br, m) ν_{as} C–O–C, 1113 (br, m) imide, 1015 (w) aromatic ring, 722 (s) δ imide. ^{1}H NMR (pyridine-d_5, δ ppm): 8.17–8.04 (6.2H), 7.93–7.90 (3.6H), 7.33–7.30 (3.6H), ~7.22 (theoretically 0.1H, overlapped).

6FDA–8ODA–2DANT (film, cm^{-1}): 3497 (vw) ν_{as} N–H, 3075 (br, w) aromatic δ C–H, 1786 (m) ν_{as} C=O, 1728 (s) ν_s C=O, 1599 (w) aromatic ring, 1502 (s) aromatic ring, 1381 (m) ν C–N, 1298 (m) ν_s CF_3, 1244 (br, m) ν_{as} C–O–C, 1109 (br, m) imide, 1015 (w) aromatic ring, 723 (s) δ imide. ^{1}H NMR (pyridine-d_5, δ ppm): 8.49–8.44 (0.4H), 8.27–8.04 (6.4H), 7.93–7.90 (3.2H), 7.77–7.71 (0.3H), 7.33–7.30 (3.2H).

6FDA–9ODA–1DANT (film, cm^{-1}): 3491 (w) ν_{as} N–H, 3070 (br, w) aromatic δ C–H, 1785 (m) ν_{as} C=O, 1729 (s) ν_s C=O, 1598 (w) aromatic ring, 1501 (s) aromatic ring, 1378 (m) ν C–N, 1297 (m) ν_s CF_3, 1256 (br, m) ν_{as} C–O–C, 1113 (br, m) imide, 1015 (w) aromatic ring, 722 (s) δ imide. ^{1}H NMR (pyridine-d_5, δ ppm): 8.49–8.44 (0.4H), 8.27–8.04 (6.4H), 7.93–7.90 (3.2H), 7.77–7.71 (0.3H), 7.33–7.30 (3.2H).

2.4. Polyimide membranes

Polymers were dissolved in THF to form 5 w/v % solutions. PTFE syringe filters (pore size 0.45 μm) were used to filter the solutions before casting membranes on glass plates at room temperature. The glass plates were placed in a dry clean chamber to avoid the contamination of dusts and to slow the evaporation of the solvent THF. Because of the worse solubility of 6FDA–ODA in THF, the THF solution 5 w/v % could not be obtained for 6FDA–ODA. In this case, pyridine, as an alternative solvent, was used as the solvent instead. The glass plate cast with 6FDA–ODA/pyridine was kept in a clean oven with a temperature of 40 °C. Transparent light brown membranes were prepared from the procedures above and were easily peeled off from the glass plates. The thicknesses of the dense membranes were 8–15 μm.

2.5. Pure gas permeation

Gas permeation tests for N_2, O_2, H_2 and He were performed at room temperature followed by CO_2 permeation with the same membranes. Membranes were placed on the porous plate in the permeation cell with an effective area of 2.38×10^{-3} m^2. Pure gases permeated through the membranes from the feed side to the permeate side. Feed gas was controlled at specific pressures (0.14, 0.21, 0.28 and 0.35 MPa), while the permeate side was kept at atmospheric pressure and permeation rates were decided by a bubble flow meter. At least 1 h purging of permeates was allowed to guarantee a steady state for the pressure changes. Permeance was calculated from Eq. (1):

$$J = \frac{q(\mathrm{STP})}{S\Delta P} \tag{1}$$

where J is the permeance in GPU, 10^{-6} (cm^3(STP))/(s cm^2 cmHg) (1 GPU = 7.5×10^{-12} m^3(STP)m^{-2} s^{-1} Pa^{-1}), q(STP) is the volumetric flux (cm^3 s^{-1}) at standard conditions which has passed through a membrane with the effective area S (cm^2), and pressure gradient across the membrane is expressed in ΔP (cmHg).

Ideal separation factor is defined as the permeance ratio of two pure gases through the same membrane, as illustrated in Eq. (2):

$$\alpha_{i/j} = \frac{J_i}{J_j} \tag{2}$$

where $\alpha_{i/j}$ is the ideal separation factor for pure gases i and j, and J_i and J_j are the permeances for pure gases i and j, respectively.

2.6. Pervaporation tests

Pervaporation was carried out for pure water permeation and dehydration of isopropanol with the same membranes. The feed temperature was controlled within ±0.2 °C with a heating mantle, Dyna-Sense® Thermoregulator Control System, a thermometer and a circulation pump (March Mfg. Inc., Model BC-2CP-MD). The circulation pump fed solutions to the membrane cell at the feed side and a vacuum (<300 Pa absolute) was applied to the other side of the membrane. Permeates were collected in cold traps with liquid nitrogen. Feed and permeate concentrations were determined by a Varian CP-3800 Gas Chromatograph. Permeation flux is defined by the following equation:

$$F = \frac{Q}{St} \tag{3}$$

where F, Q, S, t are permeation flux, total amount of permeate, membrane area and operating time, respectively.

Pure water permeation was conducted in pervaporation processes at 30, 40, 50, and 60 °C followed by dehydration of isopropanol. Temperature and concentration effects on pervaporation properties were studied in the following procedures: firstly, feed temperatures were controlled to vary from 30 to 60 °C while feed water content was kept to be ~20 wt.%. Secondly, the feed temperature was remained at 60 °C and the feed water contents were changed from ~10 to ~50 wt.%. Before samples were collected for analysis, pervaporation was operated for at least 1 h to attain steady states.

3. Results and discussion

3.1. Synthesis of polyimides

Fig. 2 illustrates the polymerization of 6FDA–8ODA–2DAPy. In addition to DAPy, DBSA, DABA and DANT were also used as the third monomer in the preparation of 6FDA–ODA-based copolyimides using the same method. The one-pot polymerization method used for the synthesis of polyimides is the one-step high-temperature polycondensation. Its application is critically limited by the solubility of the products [13]. Especially for those polyimides with a rigid structure, they may coagulate or precipitate from the reaction solutions. Therefore, the rigid structure and poor solubility may lead to low molecular weight. In one-step polycondensation, dianhydrides react with diamines in *m*-cresol at a low temperature (~80 °C) to form polyamic acids, thereafter at a high temperature (>180 °C), cyclodehydration reaction occurs with the catalyst isoquinoline to form polyimides.

Fig. 3 shows ^{1}H NMR spectra of the polyimides. The coupled peaks at 7.91 and 7.31 ppm belong to the protons of ODA moieties. For 6FDA–6ODA–4DBSA, at 8.51 ppm, a peak appears for the proton attached to α-C of the sulfonic acid group,

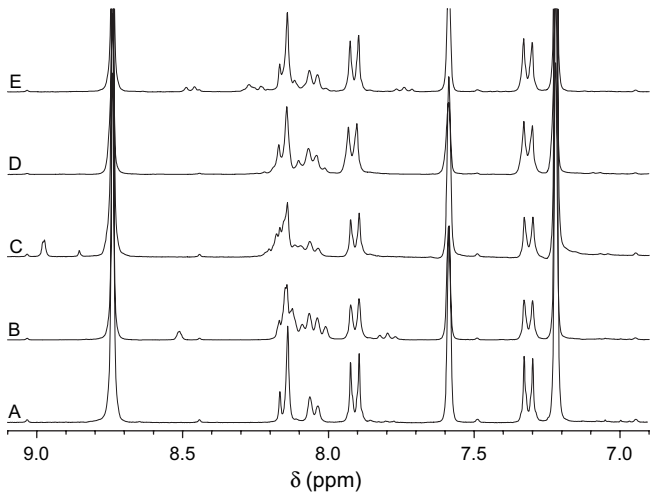

Fig. 3. ^{1}H NMR spectra of polyimides. A: 6FDA–ODA, B: 6FDA–6ODA–4DBSA, C: 6FDA–6ODA–4DABA, D: 6FDA–8ODA–2DAPy, E: 6FDA–8ODA–2DANT.

and for 6FDA–6ODA–4DABA, the proton attached to α-C of the carboxylic acid group has a chemical shift of 8.98 ppm. In ^{1}H NMR spectrum of 6FDA–8ODA–2DAPy, the resonance peaks of protons in pyridine moieties shift to ~8.15 ppm (from 7.22 ppm in pyridine) and ~7.22 ppm (from 7.59 ppm in pyridine), respectively. The protons in naphthalene moieties can be found to show chemical shifts of 8.46, 8.25 and 7.74 ppm, respectively, in ^{1}H NMR spectrum of 6FDA–8ODA–2DANT.

In FTIR spectra of the polyimides, a weak absorption band can be found at ~3494 cm^{-1}, which may indicate the existence of primary amino groups. These amino groups may be the end groups of the polyimide chains from diamine monomers, resulting from their low molecular weights. At ~3070 cm^{-1}, aromatic C–H stretching band occurs. Skeletal stretching of aromatic rings produces absorption at ~1600 cm^{-1} and ~1500 cm^{-1}, and the weak absorption at 1015 cm^{-1} is due to the in-plane bending of the phenyl rings [14]. The absorptions at 1785 cm^{-1} (C=O asymmetrical stretching, Imide I band), 1728 cm^{-1} (C=O symmetrical stretching, imide II band), 1110 cm^{-1} (imide III band), and 723 cm^{-1} (imide ring bending vibration, imide IV band), as well as 1380 cm^{-1} (C–N stretching) are characteristic absorptions of imide rings [15–17]. Asymmetrical stretching vibration of $-CF_3$ groups produces absorption at ~1300 cm^{-1}. The ether bond in ODA moieties shows strong stretching absorption at ~1240 cm^{-1}.

Table 1 exhibits molecular weights and polydispersity indexes ($\overline{M}_w/\overline{M}_n$) of the polyimides. 6FDA–8ODA–2DAPy and 6FDA–9ODA–1DAPy show lower molecular weights, while 6FDA–8ODA–2DBSA, 6FDA–6ODA–4DBSA and 6FDA–6ODA–4DABA have higher molecular weights. It is known that the rate of polycondensation is favored by the increased electron affinity of the dianhydrides and by the increased basicity of the diamines [1,13,18]. In this experiment, five diamine monomers were used in the synthesis of polyimides. The basicity of diamines was compared with the charges on the N atom of the $-NH_2$ groups. Their Wang–Ford charges obtained from MOPAC are in the following order: ODA (−0.940) > DABA (−0.930) > DANT (−0.920) > *p*-DBSA (−0.824) > DAPy (−0.760) > *o*-DBSA (−0.681). This sequence indicates the lower reactivity of the amino groups in DAPy moieties and the higher reactivity of those in DABA moieties, which results in the lower and the higher molecular weights, respectively. These polyimides show narrow molecular weight distributions. $\overline{M}_w/\overline{M}_n$ for 6FDA–ODA, 6FDA–6ODA–4DBSA, 6FDA–8ODA–2DANT and 6FDA–9ODA–1DANT are ~1.1, and 1.30–1.43 for the others. The small values of $\overline{M}_w/\overline{M}_n$ obtained from GPC probably resulted from the aggregation of polyimide chains in the polymerization solvent or in the GPC solvent [19].

3.2. Properties of polyimides

3.2.1. Solubility

Solubility of polyimides was tested by putting small pieces of polyimides into large amounts of solvents. All polymers are

readily soluble in THF and pyridine, and are also soluble in chloroform, *N*,*N*-dimethylacetamide (DMAc), *N*,*N*-dimethylformamide (DMF), *N*-methylpyrrolidone (NMP), acetone, and dimethyl sulfoxide (DMSO), but they are insoluble in isopropanol, toluene and cyclohexane. High concentration of THF solution (>3 w/v%) was unable to be prepared for 6FDA–ODA, so when casting membranes, pyridine was used as the solvent.

3.2.2. Thermal properties

Thermal analysis provides information on thermal properties of materials and offers an alternative way to study their chemical compositions and structures. In this work, DSC and TGA traces were recorded in helium at 250–370 °C and 100–650 °C, respectively, with a heating rate of 10 °C/min. Characteristic temperatures read from DSC and TGA curves are listed in Table 2. Characteristic decomposition temperatures were determined as the peak temperature in derivative thermogravimetry (DTG) plots.

From free volume theory, glass transition occurs when the expansion rate of the free volume changes, and it is reflected in the density change of a material, while in thermal analysis, glass transitions appear to be changed in heat capacities [20]. However, in this work, the glass transitions of 6FDA–ODA–based polyimides were not observed in their first and second runs of DSC. But the glass transition temperature (T_g) of 6FDA–ODA was determined to be 285.6 °C, when the DSC curve is subtracted by a baseline obtained from an empty sample pan. This T_g value is very close to the bibliographic data [13]. Furthermore, the onset temperature from the modified DSC curve of 6FDA–ODA is close to the T_g. Based on this fact, the onset temperatures of the modified DSC curves are utilized as an estimation of glass transition temperatures for polyimides. The results are listed in Table 2. 6FDA–8ODA–2DANT shows the highest onset temperature because the rigid naphthalene structure increases the transition temperature. The sulfonic acid groups of DBSA moieties and carboxylic acid groups of DABA moieties change the packing densities of the polymer chains, which may result in a slight decrease in the onset temperatures from that of 6FDA–ODA.

TGA plots record the weight change of the materials when they are heated at a specific rate. 5% and 10% weight loss temperatures are usually used to characterize the thermal stability of a material. The derivative of the TGA curves, i.e. DTG, depicts the rate of pyrolysis. TGA and DTG curves of the polyimides are exhibited in Fig. 4. DANT moieties contribute to the better thermal stability of 6FDA–8ODA–2DANT. The T_d 5% and T_d 10% of the polyimides demonstrate a sequence of thermal stability for the diamine moieties: DANT > DAPy > ODA > DBSA > DABA. The thermal

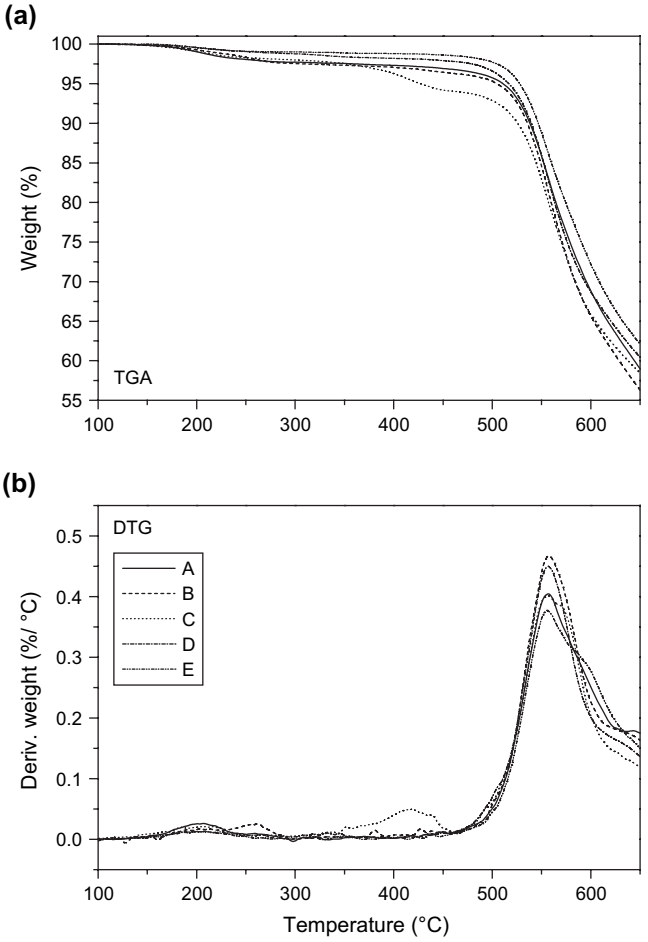

Fig. 4. TGA and DTG curves of polyimides. A: 6FDA–ODA, B: 6FDA–6ODA–4DBSA, C: 6FDA–6ODA–4DABA, D: 6FDA–8ODA–2DAPy, E: 6FDA–8ODA–2DANT.

Table 2
Characteristic temperatures from DSC, TGA and DTG

Polyimides	DSC[a] (°C)	T_d 5% wt. loss (°C)	T_d 10% wt. loss (°C)	T_d onset[c] (°C)	DTG[e] (°C)
6FDA–ODA	293.5, 285.6[b]	510.9	538.2	520.9	556.5
6FDA–6ODA–4DBSA	293.2	504.8	535.7	521.9	557.0
6FDA–6ODA–4DABA	291.2	427.4	525.8	372.2[d], 523.6	417.8[d], 556.5
6FDA–8ODA–2DAPy	294.7	516.7	539.4	519.9	556.7
6FDA–8ODA–2DANT	299.3	527.9	546.6	521.8	555.3

[a] DSC operating conditions: 10 °C/min in helium. Glass transition temperatures were not distinctly decided from the first and second runs of DSC. The onset temperatures were used as an estimation of their glass transition temperatures.
[b] Glass transition temperature of 6FDA–ODA.
[c] TGA operating conditions: 10 °C/min in helium.
[d] 6FDA–6ODA–4DABA showed two degradation stages in TGA. This temperature was obtained from the first stage degradation.
[e] These temperatures were read as DTG peak temperatures.

stability is greatly affected by the side groups of sulfonic acid and carboxylic acid. The pyrolysis of carboxylic acid groups occurs at a much lower temperature (T_d onset 372.2 °C), and consequently two stages of decomposition were observed in TGA onset and DTG peak temperatures. Except 6FDA–6ODA–4DABA, the polyimides have T_d 10% about 20 °C higher than T_d 5%. Read from the DTG plots of the polyimides, the maximum rates of degradation occur at ~556 °C. In the DTG curves, 6FDA–ODA shows a small peak at ~640 °C and the –COOH decomposition peak is found at 417.8 °C for 6FDA–6ODA–4DABA.

3.2.3. Surface free energies

Contact angles of liquid drops on horizontal membrane surfaces (sessile drops) were captured with a camera at room temperature. The values of contact angles were obtained from analysis of their shapes, and the results are presented in Table 3.

Van Oss et al. defined the surface free energy as the sum of the Lifshitz–van der Waals apolar (LW) component γ_i^{LW} and the Lewis acid–base (AB) component γ_i^{AB} [21].

$$\gamma_i = \gamma_i^{LW} + \gamma_i^{AB} \tag{4}$$

$$\gamma_i^{AB} = 2\sqrt{\gamma_i^- \gamma_i^+} \tag{5}$$

Lifshitz–van der Waals component γ_i^{LW} is the apolar component related to Lifshitz–van der Waals interactions including London dispersion forces, Debye polarization and Keesom forces, and it can be determined from measurement of the contact angles of an apolar liquid on the solid surface. The acid–base component γ_i^{AB} is associated with the acid–base interactions including hydrogen bonding, π bonds and ligand formation in a bipolar system. It was split into two mono-polar surface parameters: Lewis acid (electron-acceptor) subcomponent γ^+ and Lewis base (electron-donor) subcomponent γ^-. The substance is considered to be apolar if both the acidic and basic subcomponents are negligible. The Young equation was combined with the Dupre equation to yield [22]:

$$\gamma_l(1+\cos\theta) = \gamma_s + \gamma_l - \gamma_{sl} = -\Delta G_{sl}^{IF} \tag{6}$$

As shown in Eq. (7), the interfacial free energy was related to the individual surface free energies [23].

$$\gamma_{sl} = \gamma_{sl}^{LW} + \gamma_{sl}^{AB} = \left(\sqrt{\gamma_s^{LW}} - \sqrt{\gamma_l^{LW}}\right)^2 + 2\left(\sqrt{\gamma_s^+\gamma_s^-} + \sqrt{\gamma_l^+\gamma_l^-} - \sqrt{\gamma_s^+\gamma_l^-} - \sqrt{\gamma_s^-\gamma_l^+}\right) \tag{7}$$

In this work, γ_s^{LW} of membranes was calculated from contact angles with the apolar liquid diiodomethane (DIM). Water, glycerol and formamide were also applied in the measurement of contact angles on the polyimide membranes, and accordingly γ_s^+ and γ_s^- were decided [24].

Free energy of the interfacial interaction ΔG_{sl}^{IF} was obtained from Eq. (6) by substituting appropriate expressions [24]:

$$\Delta G_{sl}^{IF} = -2\left(\sqrt{\gamma_s^{LW}} - \sqrt{\gamma_l^{LW}}\right)^2 - 4\left(\sqrt{\gamma_s^+\gamma_s^-} + \sqrt{\gamma_l^+\gamma_l^-} - \sqrt{\gamma_s^+\gamma_l^-} - \sqrt{\gamma_s^-\gamma_l^+}\right) \tag{8}$$

Contact angles of the polyimide membranes are seen in an order for different liquids: water > glycerol > formamide ≫ diiodomethane. Since diiodomethane is considered as an apolar liquid, the smaller values of contact angles with diiodomethane reflect more affinity of the polyimides to the apolar liquid, and at the same time, the larger values of contact angles with water reflect hydrophobicity of the membranes.

Table 4 exhibits the results of membrane surface free energies and water–membrane interfacial free energies from the calculations. The values of Lifshitz–van der Waals components γ_s^{LW} appear to be in the range of 41–46 mJ/m^2 and they make the predominant contributions to the total

Table 3
Contact angles of liquids on polyimide membranes from the sessile drop method

Polymers	Water (°)	Glycerol (°)	Formamide (°)	Diiodomethane (°)
6FDA–ODA	77.5 ± 1.0	67.4 ± 2.4	54.3 ± 2.0	26.0 ± 0.6
6FDA–6ODA–4DBSA	76.1 ± 0.7	60.8 ± 0.7	51.5 ± 0.6	30.0 ± 1.4
6FDA–6ODA–4DABA	77.5 ± 1.1	63.8 ± 1.4	48.4 ± 1.1	36.8 ± 2.0
6FDA–8ODA–2DAPy	77.4 ± 2.5	66.7 ± 3.1	54.8 ± 1.1	34.3 ± 1.4
6FDA–8ODA–2DANT	78.2 ± 0.9	66.6 ± 0.5	55.7 ± 1.3	29.5 ± 2.3

All results are given as means with 95% C.I.

Table 4
Surface free energy components (mJ/m^2) and membrane–water interfacial free energies (mJ/m^2) of polyimides

Polymers	γ_s^{LW}	γ_s^+	γ_s^-	γ_s^{AB}	γ_s	ΔG_{sw}^{IF}
6FDA–ODA	45.79	0.0001	6.16	0.05	45.84	−60.67
6FDA–6ODA–4DBSA	44.22	0.2072	5.49	2.13	46.35	−57.60
6FDA–6ODA–4DABA	41.18	0.4428	4.68	2.88	44.06	−56.71
6FDA–8ODA–2DAPy	42.35	0.0431	6.54	1.06	43.41	−55.05
6FDA–8ODA–2DANT	44.43	0.0063	5.97	0.39	44.82	−59.79

surface free energies of γ_s. The great difference in the values of Lewis acid–base (AB) components γ_i^{AB} mainly results from the huge deviations in the values of the electron-acceptor (Lewis acid) components γ^+. The acidity of DBSA and DABA moieties in the polymers may contribute to a larger value of the acid components γ^+, whereas the basic components γ_s^- may possibly benefit from the basicity of the DAPy moieties. If γ^+ and γ_s^-, are compared all polyimide membranes show the properties of electron-donicity, which is probably due to the residual amino groups in the polyimides. The values of γ_s are not greatly affected by the variations in the values of γ_s^{AB}, and all membranes have surface free energy between 43 and 46.5 mJ/m^2. ΔG_{sw}^{IF} can be used to compare the affinity of the membranes to water since a negative value of ΔG_{sw}^{IF} represents hydrophobicity of the surface [23]. Hence, 6FDA-based membranes are hydrophobic membranes, but 6FDA–6ODA–4DABA and 6FDA–8ODA–2DAPy show more hydrophilicity than the others.

3.3. Gas permeation properties

The gas permeation of 6FDA–ODA and the copolyimides was conducted for five gases at room temperature from 0.14 to 0.35 MPa. The average data of gas permeance (in GPU) are outlined in Table 5. Gas permeance depends on the thicknesses of membranes, but the measurement of the thicknesses can lead to great experimental errors. Therefore, ideal separation factors are used to compare the permeation properties of the membranes. Fig. 5 shows the ideal separation factors of 6FDA–ODA and four copolyimide membranes for O_2, H_2, He and CO_2 over N_2 at different pressures. It is observed that permeation selectivity is independent of pressures, and therefore, the average ideal separation factors (exhibited in Table 5) are used for all polyimide membranes in later work.

3.3.1. Gas transport mechanism

Gas permeation in polymers is governed by the solution-diffusion mechanism [25]. Sorption occurs at the upstream side of the membrane, and gas molecules diffuse through the membrane driven by the differences of partial pressures of the permeation species existing between the upstream and downstream sides of the membrane [26]. Solubility of gases in a membrane is related to their critical temperatures. Gases with higher critical temperatures are much easier to be condensed and are more soluble in the membrane [5]. Based on the difference of their critical temperatures: CO_2 (304.1 K) > O_2 (154.6 K) > N_2 (126.2 K) > H_2 (33.2 K) > He (5.19 K), the solubility selectivity O_2/N_2 can be achieved at 1.35–1.89 in polymers at room temperature [5]. But from experimental data, α_{O_2/N_2} is in the range of 3.6–7.3 for the polyimide membranes. Hence, diffusivity difference plays a significant role in the permeation selectivity of O_2/N_2.

In the non-porous membrane, gas molecules move through the transient gaps produced from the segmental movement of the polymer matrix [5,27]. The transient gaps are related to the free volume according to the free volume theory [26]. Polymer chains in glassy polymers are strictly confined in the matrix and the whole matrix acts as a molecular sieve in gas separations. The diffusion selectivity of O_2/N_2 can be achieved up to 5 by rigid glassy polymers [5]. Considering the difference of the kinetic diameters of the gases, N_2 (0.364 nm) > O_2 (0.346 nm) > CO_2 (0.33 nm) > H_2 (0.289 nm) > He (0.26 nm) [27], H_2 and He are supposed to have much higher diffusivity selectivity than O_2. Experimental results show $\alpha_{He/N_2} > \alpha_{H_2/N_2} > \alpha_{O_2/N_2}$, and for all membranes, α_{CO_2/N_2} has values much higher than α_{O_2/N_2}, resulting from the higher critical temperature of CO_2 (304.1 K) and hence the higher solubility in polymers.

3.3.2. Moiety contributions

In addition to the solubility and diffusivity effects from gases, the intrinsic and physical properties of polymers also play a critical role in deciding the selectivity of gas pairs. Relationships between polymer structures and gas separation performances were investigated by some researchers [1,28], but they were not quantitatively described from the effects of functional groups and polymer chains. Fortunately, group contribution methods for prediction of gas permeabilities were developed [29–31]. In this work, from the ideal separation factors of 6FDA-based polyimide membranes, linear contributions of monomer moieties were proposed for α_{O_2/N_2}, α_{He/N_2}, α_{H_2/N_2} and α_{CO_2/N_2}, respectively. The linear moiety contribution method is expressed as follows:

$$f = \sum_i a_i X_i + \sum_j b_j Y_i \tag{9}$$

Table 5
Gas separation properties of polyimide membranes at room temperature

Polyimides	Permeances[a] (GPU)					Ideal separation factors			
	J_{N_2}	J_{O_2}	J_{H_2}	J_{He}	J_{CO_2}	α_{O_2/N_2}	α_{H_2/N_2}	α_{He/N_2}	α_{CO_2/N_2}
6FDA–ODA	0.03	0.14	0.99	1.26	1.45	5.1	35.5	44.9	52.0
6FDA–8ODA–2DBSA	0.02	0.14	0.95	1.07	1.34	5.5	38.8	43.3	54.3
6FDA–6ODA–4DBSA	0.02	0.13	1.40	1.90	0.90	6.0	63.9	85.0	40.2
6FDA–8ODA–2DABA	0.02	0.13	1.69	1.54	1.16	5.7	75.4	68.9	51.7
6FDA–6ODA–4DABA	0.03	0.20	0.58	2.10	0.95	7.3	21.5	74.3	35.2
6FDA–9ODA–1DAPy	0.02	0.07	0.38	0.44	0.86	3.6	18.8	21.8	42.5
6FDA–8ODA–2DAPy	0.05	0.22	2.24	3.25	1.83	4.5	50.2	67.6	38.1
6FDA–9ODA–1DANT	0.03	0.14	0.93	1.07	1.51	4.8	32.2	37.1	55.6
6FDA–8ODA–2DANT	0.02	0.10	0.54	0.60	1.35	4.7	24.8	27.6	61.9

[a] Average data of gas permeances at 0.14, 0.21, 0.28 and 0.35 MPa. 1 GPU = 7.5×10^{-12} m^3(STP) m^{-2} s^{-1} Pa^{-1}.

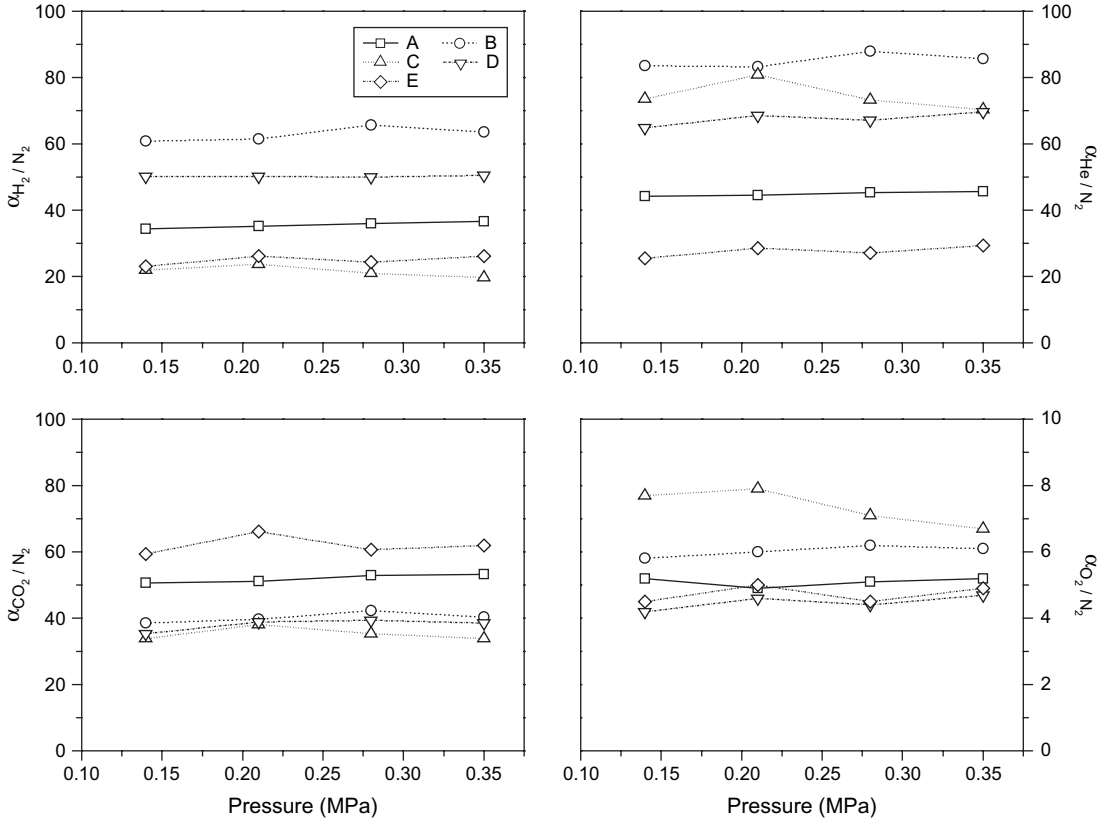

Fig. 5. Ideal separation factor of gas pairs for membranes at different pressures. A: 6FDA−ODA, B: 6FDA−6ODA−4DBSA, C: 6FDA−6ODA−4DABA, D: 6FDA−8ODA−2DAPy, E: 6FDA−8ODA−2DANT.

where $\sum_i a_i = 1$, $\sum_j b_j = 1$, and f is the dependent parameter for a membrane process, a_i and b_j are molar fractions of dianhydride moieties and diamine moieties, respectively, X_i and Y_j are moiety contribution factors for dianhydride moieties and diamine moieties, respectively. Results from least square regression of ideal separation factors of gas pairs (as shown in Table 5) are listed in Table 6.

Molecular sieving effect on the non-condensable gases of O_2, He and H_2 can be seen from the contributions of monomer moieties. Moieties of 6FDA, DBSA and DABA contribute positively to the selectivities of gas pairs O_2/N_2, He/N_2 and H_2/N_2, and their contributions are enhanced by the size differences of gas molecules. Though DAPy moiety has a negative value for O_2/N_2, it still behaves in the same way for He/N_2 and H_2/N_2 as 6FDA, DBSA and DABA moieties. The $-CF_3$ groups in 6FDA, $-SO_3H$ groups in DBSA and $-COOH$ groups in DABA occupy more space in the matrices, and polymer chains can pack more loosely [32]. Gas molecules of smaller sizes and lower solubility in the membrane can easily pass through, resulting in a higher selectivity against N_2. The smaller size and more rigid structure of DAPy moiety decrease the mobility of O_2 (possibly N_2 as well), but the mobility of He and H_2 is not greatly affected, and at the same time the distribution concentration of 6FDA moieties is enhanced by the introduction of DAPy. ODA moiety behaves inversely because it decreases the effects of 6FDA moieties in the main chain, in spite of a positive contribution merely favorable to the diffusion of O_2 other than N_2, probably due to the flexible ether bond. DANT moiety is different from the others: the rigid naphthalene structure that is larger than DAPy moiety may produce more space for O_2, but it may limit the mobility of H_2 and He in the polymer matrix. The contributions of monomer moieties for α_{CO_2/N_2} reflect their overall influences on CO_2 solubility and diffusivity in the polymers. It is interesting that the existence of pyridine structure with the Lewis base property decreases α_{CO_2/N_2}. The lone electron pair may be the cause of the solubility change of CO_2 in the polymers.

Table 6
Contributions of monomer moieties to the ideal separation factors

Moieties of monomers	α_{O_2/N_2}	α_{H_2/N_2}	α_{He/N_2}	α_{CO_2/N_2}
6FDA	3.6	29.4	36.4	33.8
ODA	0.6	−0.4	−2.7	9.6
DBSA	5.9	79.5	101.2	13.2
DABA	8.2	31.1	113.6	1.5
DAPy	−2.9	20.7	58.8	−28.4
DANT	3.6	−10.6	−20.5	108.0

Values were calculated from 6FDA-based polyimides using least square regression method. Calculations should be based on the overall molar ratio of dianhydrides/diamines of 1:1.

Fig. 6 shows the comparison of the experimental data with the calculated ideal separation factors for the polyimide membranes. The calculated α_{O_2/N_2} and α_{CO_2/N_2} can fit better than

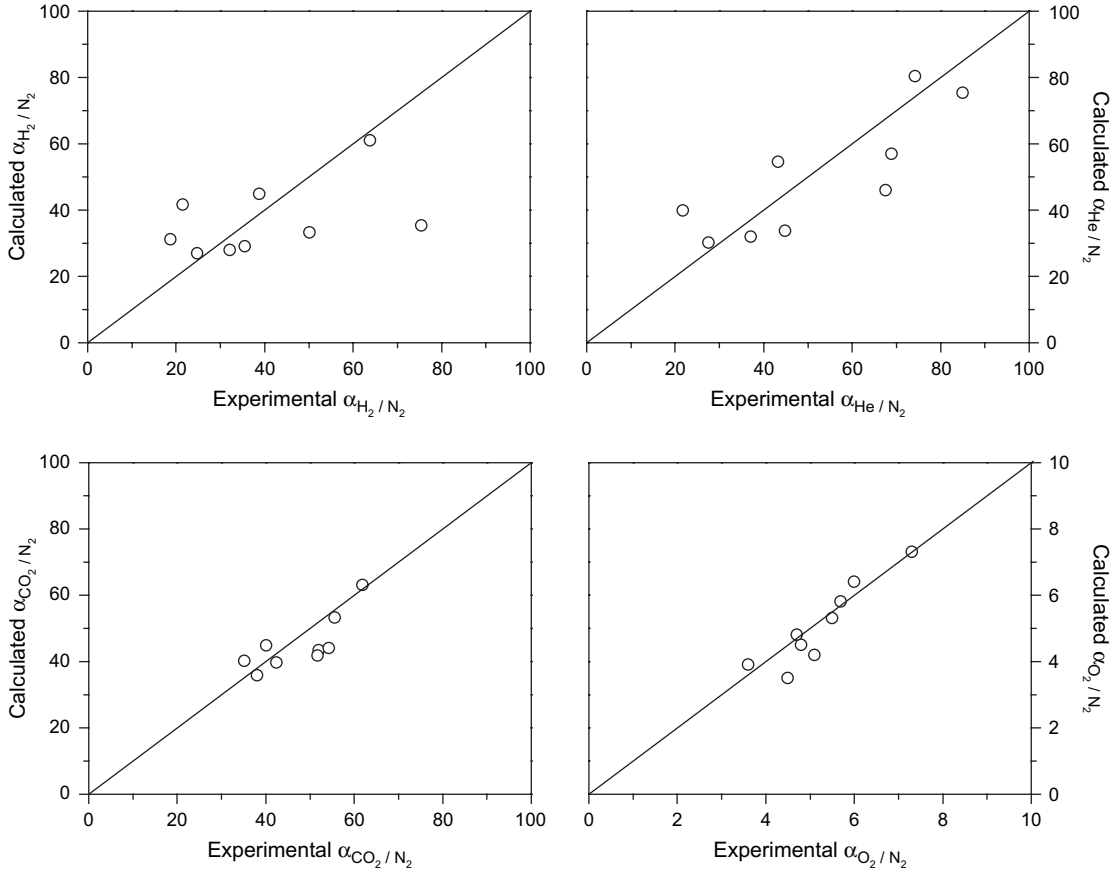

Fig. 6. Comparison of experimental ideal separation factors with the calculated values for polyimide membranes.

α_{He/N_2} and α_{H_2/N_2}. More data are required for more accurate predictions from this method.

3.4. Pervaporation properties

Pervaporation experiments were carried out for pure water permeation and dehydration of isopropanol. Temperature and feed concentration dependencies of permeation flux and selectivity were studied with a feed water content ~20 wt.% at 30–70 °C and feed water contents 10–50 wt.% at 60 °C, respectively. Permeation flux of water at 30–70 °C was also obtained from the experiments.

3.4.1. Mass transport mechanism

In pervaporation, the liquid components of the feed mixture selectively permeate through the membrane, and the process yields a vaporous product with the aid of vacuum or the purge gas at the permeate side. The mass transport is governed by the widely accepted solution-diffusion mechanism [26]. Sorption occurs at the feed side surface of the membrane, and the penetrants diffuse across the membrane followed by evaporation/desorption of the components into the permeate side with a lower partial pressure [33]. Desorption is usually considered as a fast step [26], so sorption/solution and diffusion properties of the penetrants in the membrane are of great importance.

As discussed for gas separation, the molecular sizes of the penetrants and the dimension of the transport paths from thermal transient gaps in the membranes are critical parameters that are used to determine the diffusivity of the penetrants in glassy polymers. In this case, isopropanol has a molecular diameter (0.43 nm) much larger than water (0.265 nm) [27,34], which can cause the lower diffusivity of isopropanol compared with water. The high glass transition temperatures and the rigidity of aromatic imide moieties result in the low mobility of the segmental chains of the polyimides, thereby restricting the diffusivity of isopropanol and water. As another factor influencing the diffusivity of penetrants, packing properties of the polyimide matrices are attributed to the regularity of the polymer chains as well as the steric effects of side groups [32]. DAPy and DANT moieties in the copolyimides change the regularity of the polymer chains, and in addition, DABA and DBSA moieties bearing bulky groups, help to improve the diffusivity of the penetrants. Besides the steric effects, the pyridine moiety (in DAPy) and the functional groups, such as sulfonic acid (in DBSA) and carboxylic acid (in DABA) groups, may have some favorable diffusional effects derived from their physiochemical interactions with isopropanol and/or water. Furthermore, such interactions can possibly change the physical properties of the polymer matrices, such as packing densities and glass transition temperatures. As a matter of fact, most of these interactions are

essentially related to the solubility of the penetrants in the polymers, or in other words, the sorption properties of the membranes.

Sorption of the penetrants in polymer membranes can be considered as the formation of polymer solutions where the polymers are ''solvents'' for the penetrants. Functional groups play important roles in sorption properties because of their interactions with the penetrants. The acyl groups in imide rings can form hydrogen bonds with water, and the hydrophilic groups such as sulfonic acid group and carboxylic acid group are favorable to the sorption of water. However, the pyridine moiety may have a positive effect on isopropanol, and the aromatic properties of the polyimide membranes may promote the solubility of isopropanol. In 6FDA-based polyimides, $-CF_3$ shows unfavorable effects on the solubilities of the penetrants, but it is beneficial to the flexibility of polymer matrices and can cause higher diffusivity.

3.4.2. *Effects of functional groups on selectivity*

Polyimide membranes show good selectivity for water. As shown in Fig. 7, most membranes have water contents in permeates higher than 90 wt.%. It is also observed that by introducing a third monomer into the main chains of 6FDA–ODA, the selectivity of the membrane undergoes a great change considering the permeate water contents.

First of all, it should be noted that 6FDA–ODA membranes were cast from the pyridine solution, and the solvent may have some effects on the chain packing properties. Furthermore, 6FDA–ODA has better regularity in the main chain than the copolyimides and the higher packing density may lead to the lower permeation of both water and isopropanol.

DBSA and DAPy moieties have similar effects on permeation selectivity. When small amounts of DBSA and DAPy are introduced to substitute ODA, the loose packing of polymer matrices may occur because of the irregularity of the main chains. With more moieties of the third monomers, more water can selectively permeate, probably due to the higher solubility in the matrices. DABA moieties have reverse effects compared with DBSA and DAPy. Generally speaking, DABA moieties may have two effects, hydrogen bonding effect (favorable to water permeation) and size-induced steric effect (favorable to both isopropanol and water), which may cause higher water contents in permeates with a small number of DABA moieties, but lower water contents in permeates with a large number of DABA moieties in the main chains. DANT moieties in 6FDA–ODA-based copolyimides show affinity to

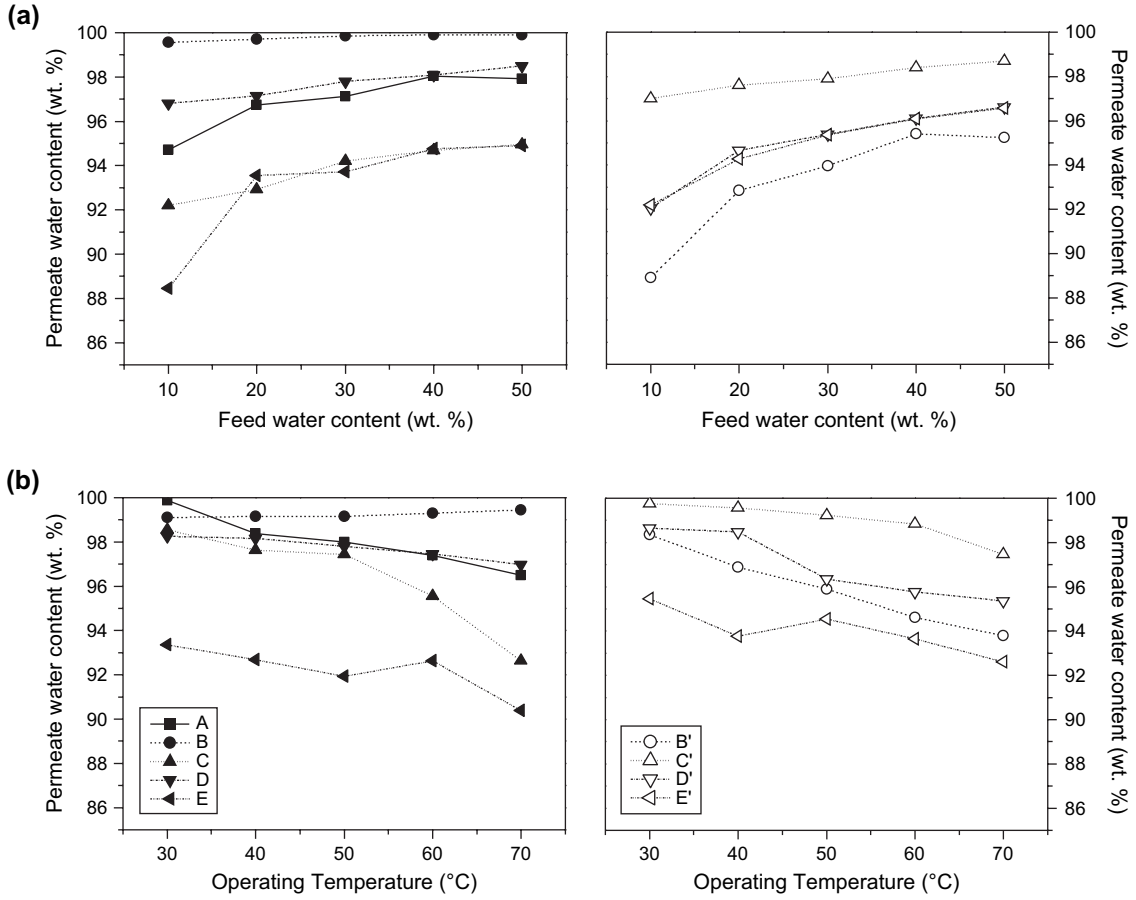

Fig. 7. Permeate water contents of polyimide membranes in pervaporation dehydration of isopropanol. A: 6FDA–ODA, B: 6FDA–6ODA–4DBSA, C: 6FDA–6ODA–4DABA, D: 6FDA–8ODA–2DAPy, E: 6FDA–8ODA–2DANT. B′: 6FDA–8ODA–2DBSA, C′: 6FDA–8ODA–2DABA, D′: 6FDA–9ODA–1DAPy, E′: 6FDA–9ODA–1DANT.

isopropanol and decrease the permeate water contents in pervaporation.

3.4.3. Effects of the feed concentration

Fig. 7 exhibits the feed concentration effects on permeate water contents in pervaporation dehydration of isopropanol. With more water in the feed, higher water contents can be observed in permeates for all membranes. Permeation flux shows an analogous tendency for all membranes.

Based on the experimental data, an empirical equation was developed from curve fitting for concentration effects on permeation flux:

$$F(x) = k\,x_w^n \left(0.1 < x_w < 0.5\right) \tag{10}$$

where $F(x)$ is the total permeation flux at a feed water content of $x_w \times 100$ wt.%, n is the concentration coefficient for total flux, k is a parameter related to the membrane material and thickness as well as operation temperatures, and it is considered to be a constant for the same membrane at the same operating temperature.

Values of n were determined from total flux through the same membranes and four data points were utilized to achieve the best regression for each membrane. Results are listed in Table 7 along with the coefficients of determination r^2. Most of the coefficients of determination are greater than 0.99, which indicates good qualities of fit achieved by the regression.

Linear contributions of monomer moieties were also calculated for concentration coefficients based on Eq. (9) and results are listed in Table 8. In Eq. (10), $0.1 < x_w < 0.5$, and a larger value of n will result in a smaller value of x_w^n. It is observed that the hydrophilic DBSA and DABA moieties have greater n values, because the sorption properties of the membranes may not change significantly considering the "fixed space" for the sorbed penetrants in glassy matrices, while for ODA moiety, sorption is enhanced with a high concentration of water in the feed, so that the total flux is improved. DANT moiety with a rigid naphthalene structure may have "less space" for the sorbed penetrants, particularly for isopropanol, and moreover, no functional groups may facilitate possible interactions with water in DANT moieties. As a result, total flux of the polyimide membranes containing DANT moieties does not increase significantly when increasing the feed water content.

Fig. 8 shows the comparison of concentration coefficients from experimental data with those from calculations. The validity of the method is confirmed from these results.

Table 7
Concentration coefficients and permeation activation energies for pervaporation

Polyimides	n (r^2)[a]	E_p (pure water)[b] (kJ/mol)	E_p (total flux)[c] (kJ/mol)
6FDA–ODA	0.22 (0.99)	15.7	46.1
6FDA–8ODA–2DBSA	0.37 (0.94)	17.7	40.9
6FDA–6ODA–4DBSA	0.39 (0.99)	36.1	37.4
6FDA–8ODA–2DABA	0.35 (0.98)	28.6	53.6
6FDA–6ODA–4DABA	0.44 (0.99)	32.1	59.6
6FDA–9ODA–1DAPy	0.33 (0.99)	31.9	49.4
6FDA–8ODA–2DAPy	0.37 (0.99)	34.0	55.6
6FDA–9ODA–1DANT	0.32 (0.92)	15.2	34.4
6FDA–8ODA–2DANT	0.36 (0.95)	12.7	30.1

[a] Curve fitting was made based on four data points to achieve the best regression for each membrane.
[b] Activation energies for pure water permeation.
[c] Activation energies for total permeation flux with feed water content ~20 wt.%.

Table 8
Moiety contributions to concentration coefficients and permeation activation energies

Moieties of monomers	n	E_p (pure water) (kJ/mol)	E_p (total flux) (kJ/mol)
6FDA	0.25	24.1	35.6
ODA	0.03	−6.7	7.1
DBSA	0.37	33.0	0.7
DABA	0.41	33.7	51.6
DAPy	0.18	98.0	27.0
DANT	0.41	−30.2	−60.3

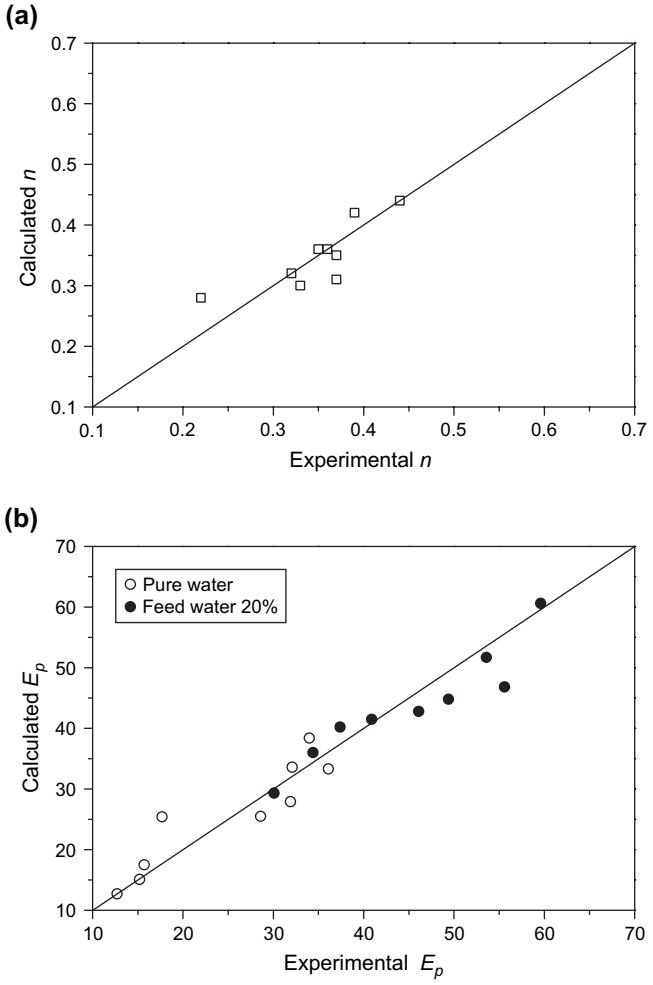

Fig. 8. Comparison of concentration coefficients and permeation activation energies from calculations of linear moiety contributions with those from experimental data.

3.4.4. Effects of the operating temperature

Fig. 7 shows the permeate water contents from pervaporation of aqueous isopropanol solutions of ~20 wt.% water in the feed. Generally speaking, temperature effect leads to a trade-off relationship between permeation flux and selectivity, i.e. the higher operating temperature, the higher flux but the lower permeate water content in the case of dehydration of isopropanol. This phenomenon can be observed in all membranes except 6FDA–6ODA–4DBSA. The trade-off relationship is supposed to be caused by the interactions of water and isopropanol with the polyimides at elevated temperatures, but still needs more evidences and further investigations.

The Arrhenius-type equation is a well-known tool to analyze the pervaporation properties at different temperatures.

$$F(T) = Ae^{-E_p/RT} \tag{11}$$

where $F(T)$ is the total permeation flux at temperature T, E_p is the permeation activation energy, R is the gas constant and A is the pre-exponential factor.

Activation energies for pure water permeation are listed in Table 7. Since the feed concentration is required to be constant in the application of Arrhenius-type equation, compensation of the feed concentrations must be made. By combining Eqs. (10) and (11), the following equation can be obtained:

$$F(T,x) = Kx_w^n e^{-E_p/RT} \tag{12}$$

where K is supposed to be a parameter related to the membrane material and the membrane thickness. It should also be noted that no experimental data were applied in finding this equation. The assumption is based on the fact that small differences in feed water contents have very weak influence on permeate water contents. Furthermore, no significant difference can be found between the results from the original data and those from the modified data. Thus, activation energies for dehydration of isopropanol with feed water content 20 wt.% were calculated and are exhibited in Table 7.

Linear moiety contributions to the activation energies were calculated based on Eq. (9) from least square regression, and the results are presented in Table 8. It is much more complicated to study the effects of functional groups/moieties on permeation activation energies because temperature can not only increase the mobility of the segmental chains of polymers, but also change the sorption properties. In some cases, sorption properties may be crucial for permeation flux. The moiety contributions to activation energies appear to be in the following sequences (negative signs included) for pure water permeation: DAPy > DABA > DBSA > 6FDA > ODA (−) > DANT (−) and for total flux: DABA > 6FDA > DAPy > ODA > DBSA > DANT (−). The negative contributions from DANT indicate that the effects of the rigid structure offset the flux increase caused by the moieties of 6FDA and ODA in the main chain. A great discrepancy is observed in the contributions of DBSA to the activation energies of pure water permeation and total flux, which may result from the interactions between isopropanol and DBSA moieties. Shrinkage of the polymer matrices may occur when introducing DBSA moieties to the polyimides, and may offset the positive effect from the increase of segmental mobility at elevated temperatures, leading to lower flux but higher selectivity. As seen in Fig. 7, when increasing operating temperature, 6FDA–6ODA–4DBSA shows higher selectivity and higher flux as well.

Permeation activation energies were calculated from the linear contribution method and they are compared with those from the experimental data, as seen in Fig. 8. The reasonableness of the linear contributions from monomer moieties is suggested by the agreement between the experimental results and the calculated results.

4. Conclusions

Copolyimides of high molecular weights were prepared from one-step high-temperature polymerization of 6FDA and ODA with four diamines DBSA, DABA, DAPy and DANT as the third monomers. Their chemical structures and compositions were confirmed by FTIR and NMR spectra. The polyimides showed good thermal stabilities in DSC and TGA.

Surface free energies and membrane–water interfacial free energies were calculated from contact angles, and it was found out DABA, DBSA and DAPy moieties helped to increase the hydrophilicity of 6FDA–ODA-based membranes.

Gas permeation was measured for N_2, O_2, H_2, He and CO_2. Linear moiety contribution method was proposed to study the moiety effects on gas selectivities. Introduction of third monomers in 6FDA–ODA main chains increased their rigidity and limited the segmental mobility, but the side groups in DABA and DBSA provided more space for gas transport due to the loose packing of polymer chains. Permeabilities of N_2, O_2, H_2 and He and the corresponding selectivities were greatly affected by the steric effects of the monomer moieties, but the permeation of CO_2 was controlled by its solubility in the polymers as well as the interactions with the functional groups.

Water permeation and dehydration of isopropanol were carried out in pervaporation processes. Concentration coefficients were proposed for feed concentration effects on permeation flux, and permeation activation energies were used to study the operating temperature dependence of flux. Linear moiety contribution method was applied in order to quantitatively compare the influences of monomer moieties on these parameters. Chemical structures of the monomers, especially functional groups, could change the sorption and diffusion properties. From comparison of the moiety contribution factors, it was concluded that sorption properties were affected when changing the feed concentration, and temperature effects led to changes in diffusion properties of the penetrants.

Acknowledgement

We would like to thank the Natural Sciences and Engineering Research Council (NSERC) of Canada for its financial support.

References

[1] Ohya H, Kudryavtsev VV, Semenova SI, editors. Polyimide membranes, applications, fabrications, and properties. Amsterdam: Gordon and Breach Publishers; 1996.
[2] Huang RYM, Feng X. Sep Sci Technol 1992;27:1579–83.
[3] Zhou F, Koros WJ. Polymer 2006;47:280–8.
[4] Qiao X, Chung T-S, Pramoda KP. J Membr Sci 2005;264:176–89.
[5] Koros WJ, Fleming GK. J Membr Sci 1993;83:1–80.
[6] Okamoto K, Tanihara N, Watanabe H, Tanaka K, Kita H, Nakamura A, et al. J Membr Sci 1992;68:53–63.
[7] Kang YS, Jung B, Kim UY. Mol Cryst Liq Cryst 1993;224:137–46.
[8] Piroux F, Espuche E, Mercier R, Pineri M, Gebel G. J Membr Sci 2002; 209:241–53.
[9] Tanaka K, Islam MN, Kido M, Kita H, Okamoto K. Polymer 2006;47: 4370–7.
[10] Al-Masri M, Kricheldorf HR, Fritsch D. Macromolecules 1999;32: 7853–8.
[11] Pinel E, Brown D, Bas C, Mercier R, Alberola ND, Neyertz S. Macromolecules 2002;35:10198–209.
[12] Xu W, Paul DR, Koros WJ. J Membr Sci 2003;219:89–102.
[13] Sroog CE. Prog Polym Sci 1991;16:561–694.
[14] Silverstein RM, Bassler GC, Morrill TC. Spectrometric identification of organic compounds. New York: Wiley-Interscience; 1997.
[15] Dunson DL, Synthesis and characterization of thermosetting polyimide oligomers for microelectronics packaging, PhD dissertation, Virginia Tech; 2000.
[16] Pramoda K, Liu S, Chung T-S. Macromol Mater Eng 2002;287:931–7.
[17] Sroog CE, Endrey AL, Abramo SV, Berr CE, Edwards WM, Olivier KL. J Polym Sci Part A 1965;3:1373–90.
[18] Wilson D, Stenzenberger HD, Hergenrother PM, editors. Polyimides. Glasgow and London: Blackie & Son; 1990.
[19] Wang DH, Shen Z, Guo M, Cheng SZD, Harris FW. Macromolecules 2007;40:889–900.
[20] Sperling LH. Introduction to physical polymer science. New York: John Wiley & Sons; 2001.
[21] Schrader ME, Loeb G, editors. Modern approach to wettability: theory and applications. New York: Plenum Press; 1991.
[22] Oh E, Luner PE. Int J Pharm 1999;188:203–19.
[23] Van Oss CJ, Giese RF. Clays Clay Miner 1995;43:474–7.
[24] De Bartolo L, Gugliuzza A, Morrelli S, Cirillo B, Gordano A, Drioli E. J Mater Sci Mater Med 2004;15:877–83.
[25] Baker RW. Membrane technology and applications. Chichester: John Wiley & Sons; 2004.
[26] Ho WSW, Sirkar KK. Membrane handbook. New York: Van Nostrand Reinhold; 1992.
[27] Perry JD, Nagai K, Koros WJ. MRS Bull 2006;31:745–9.
[28] Kim TH, Koros WJ, Husk GR, O'Brien KC. J Membr Sci 1988;37: 45–62.
[29] Salame M. Polym Eng Sci 1986;26:1543–6.
[30] Park JY, Paul DR. J Membr Sci 1997;125:23–39.
[31] Robeson LM, Smith CD, Langsam M. J Membr Sci 1997;132:33–54.
[32] Pandey P, Chauhan RS. Prog Polym Sci 2001;26:853–93.
[33] Shao P, Huang RYM. J Membr Sci 2007;287:162–79.
[34] Kuznicki SM, Langner TW, Curran JS, Bell VA. US Patent 6379436, 2002.